Springer Aerospace Technology

Upendra N. Singh
Georgios Tzeremes
Tamer F. Refaat
Pol Ribes Pleguezuelo *Editors*

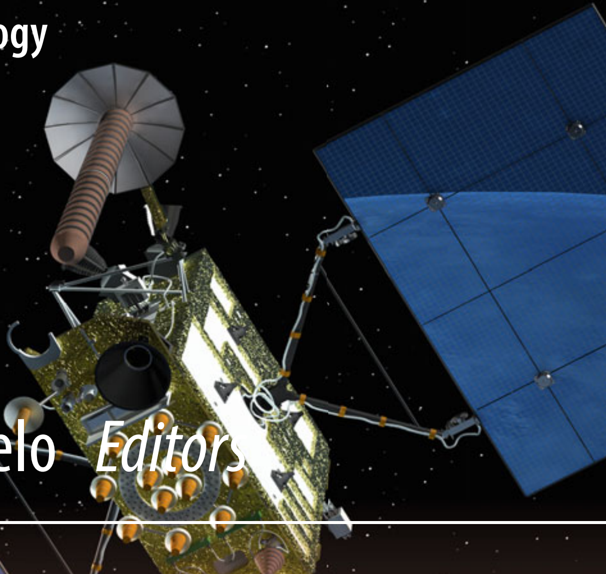

Space-based Lidar Remote Sensing Techniques and Emerging Technologies

Proceedings of the 3rd International Space Lidar Workshop

Springer

Springer Aerospace Technology

The series explores the technology and the science related to the aircraft and spacecraft including concept, design, assembly, control and maintenance. The topics cover aircraft, missiles, space vehicles, aircraft engines and propulsion units. The volumes of the series present the fundamentals, the applications and the advances in all the fields related to aerospace engineering, including:

- structural analysis,
- aerodynamics,
- aeroelasticity,
- aeroacoustics,
- flight mechanics and dynamics,
- orbital maneuvers,
- avionics,
- systems design,
- materials technology,
- launch technology,
- payload and satellite technology,
- space industry, medicine and biology.

The series' scope includes monographs, professional books, advanced textbooks, as well as selected contributions from specialized conferences and workshops.

The volumes of the series are single-blind peer-reviewed.

To submit a proposal or request further information, please contact: Mr. Pierpaolo Riva at pierpaolo.riva@springer.com (Europe and Americas) Mr. Mengchu Huang at mengchu.huang@springer.com (China)

The series is indexed in Scopus and Compendex

Upendra N. Singh · Georgios Tzeremes ·
Tamer F. Refaat · Pol Ribes Pleguezuelo
Editors

Space-based Lidar Remote Sensing Techniques and Emerging Technologies

Proceedings of the 3rd International Space Lidar Workshop

Springer

Editors
Upendra N. Singh
NASA Langley Research Center
NASA Engineering and Safety Center
Hampton, VA, USA

Tamer F. Refaat
NASA Langley Research Center
Remote Sensing Branch
Hampton, VA, USA

Georgios Tzeremes
ESA—ESTEC
Noordwijk, The Netherlands

Pol Ribes Pleguezuelo
ESA—ESTEC
Noordwijk, The Netherlands

ISSN 1869-1730 ISSN 1869-1749 (electronic)
Springer Aerospace Technology
ISBN 978-3-031-53617-5 ISBN 978-3-031-53618-2 (eBook)
https://doi.org/10.1007/978-3-031-53618-2

This Springer imprint is published by the registered company Springer Nature Switzerland AG
The registered company address is: Gewerbestrasse 11, 6330 Cham, Switzerland

Paper in this product is recyclable.

Preface

The 3rd International Workshop on Space-based Lidar Remote Sensing Techniques and Emerging Technologies was held in Milos, Greece, between June 18 and June 23, 2023. The intent of this workshop was to offer a venue and create a framework, where leaders, scientists and technologists from government agencies, academia, and industries, from different countries, can meet and discuss important issues related to current and planned lidar space missions, including techniques and associated emerging and enabling technologies. Also, it was an opportunity to discuss challenges and common issues and explore ways to increase collaboration among agencies and organizations to enhance the future social benefit of active space-based remote sensing. The workshop goals were:

- Review and assess the scientific needs for space-based lidar measurements, instrument synergies, and the maturity of lidar techniques to meet these needs.
- Introduce upcoming space-based lidar missions and present/discuss results from existing and past lidar space-based missions.
- Discuss challenges and future directions in research and technology development.
- Discuss approaches to mitigate risk and costs for space-based lidar instruments and increase mission lifetime.
- Identify synergies and ways to enhance space lidar missions through international cooperation among various space agencies and organizations.
- Document the outcome in completion and update the white paper from prior workshop.

The main topics covered by the presentations and discussion were:

- Advances in space-based lidar techniques and methodologies
- Science highlights, observational approaches, and technologies used
- Challenges experienced and lessons learned in space lidar missions to date and discussion of approaches to overcome them
- Planning of new space Earth Observation lidar missions, which include monitoring of: Topography, Cryosphere, Biomass, Greenhouse and Trace Gases Clouds, Aerosols, Oceans, and Winds

- Exploration Lidars: Entry, Decent and Precision Landing, as well as Hazard Avoidance for Mars and Lunar landers missions
- Results and plans for simulations, airborne experiments, and demonstrations as precursors for space missions
- New and emerging space lidar technologies, particularly in lasers, optics, electronics, and detectors as well as space lidar reliability and influencing factors, such as effects of the space environment (thermal, vibration, contamination, and radiation effects).

The workshop covered the following Space Lidar five sessions:

Session 1: Lidar Active Sensing (i): Topography, Cryosphere, Biomass, Gravity, Greenhouse, and Trace Gases
Session 2: Lidar Active Sensing (ii): Clouds, Aerosols, Oceans, and Winds
Session 3: Exploration Lidars: Entry/Decent/Landing, Precision Landing and Hazard Avoidance, Mars & Lunar Landers
Session 4: Ground/Airborne Campaigns for Space Lidar Cal/Val: Ground campaigns for Cal/Val, Airborne demonstration systems
Session 5: New and Emerging Space Lidar Technologies & Reliability: Laser Transmitters, Advanced Optical Components and Diffractive Optics, State-Of-The-Art Detector and Detection System, Lidar Software and Data Processing.

Thank you for attending and contributing to the workshop.

Hampton, USA — Upendra N. Singh
Noordwijk, The Netherlands — Georgios Tzeremes
Hampton, USA — Tamer F. Refaat
Noordwijk, The Netherlands — Pol Ribes Pleguezuelo

Contents

The NASA HSRL Pathfinder Mission Concept 1
Chris Hostetler, John Smith, Richard Hare, Amin Nehrir, Shane Seaman, Anthony Notari, Richard Ferrare, Sharon Burton, Kathleen Powell, Tyler Thorsen, Mark Vaughan, Johnathan Hair, Robert Holz, Willem Marais, Edwin Eloranta, and Fran Fitzpatrick

25 Years of CALIPSO 15
David Winker

AWP: NASA's Aerosol Wind Profiler Coherent Doppler Wind Lidar . . . 27
Kristopher Bedka, John Marketon, Sammy Henderson, and Michael Kavaya

Future Space-Based Coherent Doppler Wind Lidar for Global Wind Profile Observation 37
Shoekn Ishii, Kozo Okamoto, Hajime Okamoto, Toshiyoshi Kimura, Takuji Kubota, Shunsuke Imamura, Daisuke Sakaizawa, Koichi Fujihira, Ayako Matsumoto, Izumi Okabe, Tsuyoshi T. Sekiyama, Tomoaki Nishizawa, Tetsuya Takemi, Yoshiaki Miyamoto, Atsushi Sato, Riko Oki, Masaki Satoh, and Toshiki Iwasaki

A SmallSat Lidar Concept for Measurements of Aerosol and Cloud Spatiotemporal Variability 47
John Yorks, Ed Nowottnick, V. Stanley Scott, Matthew J. McGill, Patrick Selmer, Kenneth Christian, and Natalie Midzak

Towards Establishing a Long-Term Cloud Record from Space-Borne Lidar Observations 57
Artem Feofilov, Hélène Chepfer, Vincent Noël, and Maryam Hajiaghazadeh-Roodsari

Carbon Dioxide Active Remote Sensing Using Pulsed 2-μm Lidar 73
Tamer F. Refaat and Upendra N. Singh

Research and Development of the ISS Onboard Lidar Mission and Advanced Altimeter Mission 87
Daisuke Sakaizawa, Youhei Okawa, Rei Mitsuhashi, Yoshito Sawada, Tadashi Imai, and Taishi Sumita

Spaceborne Aerosol and Carbon Dioxide Detection Lidar (ACDL) Status and Progress 97
Weibiao Chen, Jiqiao Liu, Xia Hou, Huaguo Zang, Yuan Wan, Xiaopeng Zhu, Xiuhua Ma, Dijun Chen, and Rui Li

An Efficient 256-Track Beam Steering Lidar Using Wavelength-Tuning for Topography Swath Mapping from Space 109
Guangning Yang, David J. Harding, Jeffrey R. Chen, Hui Li, Erwan Mazarico, Brooke Medley, Mark A. Stephen, Xiaoli Sun, Wei Lu, Kenji Numata, Xiaozhen Xu, Kenneth J. Ranson, Philip W. Dabney, James Mackinnon, and Hannah Tomio

AIRMO: Novel Micro-lidar Powered Spectrometer for GHG Monitoring from CubeSat 119
Errico Armandillo, Daria Stepanova, and David Rees

The ESA HERA Mission and Its Planetary Altimeter—Learning to Deflect Asteroids 131
Hannah Goldberg, Pol Ribes Pleguezuelo, Ian Carnelli, Tiago Sousa, Paulo Gordo, Nicole G. Dias, Hugo Onderwater, David Hellmann, and Henning Kempfe

New Space Compact Flash Lidar 139
Jean-Christophe Roulet, David Nguyen, Christophe Meier, Antoine Ummel, Leonardo Gasparini, and Christophe Pache

Miniaturized Flash Lidar for Landing Applications 151
Steinar Johnsen, Torbjørn Grøder, Eystein Thorsvik Sæther, Benjamin Hagaas, Einar Waldrop, Anders Hauk Fritzell, Karl Henrik Haugholt, Anders Hansen, Håvard Tørring, and Baard Nossum

Evolution in Lidar Technology for Commercial Lunar Missions 165
Matias Hernandez, David Jones, Hussein Pirmohamed, Kerry Sanz, Linda Ngozwana, Steve Legate, Joshua Longstaffe, and Jack Wells

FMCW LiDAR for Lunar Descent Payload 179
Eduardo Margallo, Fabrizio Silvestri, Ivan Ferrario, Jose Luis Rubio, Ivan Bravo, and Gregory Pandraud

A Rad-Hard-by-Design TDC Chip for Today's and Future LIDARs 191
H. Marien, B. Van Bockel, S. Ali, N. Jadhav, D. Hendrickx, and Y. Cao

Prospects for Photonic Integrated Circuit LIDARs in Space Applications 203
Chrysovalantis Avraam, Tiago Sousa, Iain Mckenzie, Errico Armandillo, and Stavros Iezekiel

Photonic Integration Advancements in Miniaturizing High Reliability LIDAR System Components 213
Jes Sherman, Steven Estrella, Victoria Rosborough, Jenna Campbell, Michelle Labrecque, Brandon Isaac, Jason Seifter, Hannah Grant, Juergen Musolf, Don Kebort, Ruby Gans, Sabrina Wagner, Amin Nehrir, Gordon Morrison, Leif Johansson, and Milan Mashanovich

Heterodyne and Direct Detection Wind Lidar Developed at ONERA . . . 227
David Tomline Michel, Béatrice Augère, Thibault Boulant, Nicolas Cézard, Agnès Dolfi-Bouteyre, Anne Durécu, Didier Goular, François Gustave, Anasthase Limery, Laurent Lombard, Jean-François Mariscal, Christophe Planchat, Jonathan Pouillaude, Nicolas Rouanet, Pierre Pichon, and Matthieu Valla

EMORAL—Mobile Mie-Raman Lidar with Fluorescence, Polarization and Water Vapor Observational Capabilities for Satellite Cal/Val Field Campaigns 239
Iwona S. Stachlewska, George Georgoussis, Volker Freudenthaler, Afwan Hafiz, Patryk Poczta, Alexandros Louridas, Dongxiang Wang, Lucja Janicka, Nikolaos Siomos, Maciej Karasewicz, Rafał Fortuna, Panagiotis Kokkalis, Vassilis Amiridis, Steigvilė Byčenkienė, Anetta Drzeniecka-Osiadacz, Livio Belegante, Doina Nicolae, Georgios Tzeremes, Pol Ribes Pleguezuelo, and Dirk Schüttemeyer

Laser Development at HiLASE for Space-Based Applications 253
Martin Divoky, Jaroslav Huynh, Petr Bohacek, Jiri Muzik, Martin Smrz, and Tomas Mocek

Microchip Laser for Time of Flight Rangefinder and Lidar 259
Ana de Sousa, Bruno Couto, Paulo Gordo, Hugo Onderwater, Beltran N. Arribas, Rafael A. G. Pinto, and Rui Melicio

High-Power >20 W Single-Mode Fiber Optic Connector for LiDAR and Free-Space-Optical Communications Systems 273
Ronald T. Logan, Joesph R. Demers, and Davinder Basuita

Laser Beam Soldering of Mounts for High-Power Space Optics 281
Grucheska Rosario Rodriguez, Erik Beckert, and Thomas Peschel

FLAMES—High Speed Flash-LiDAR CMOS Imager for Landing Missions 291
Gaozhan Cai, Victor Schuddinck, Amir Babaiefishani, Koen Liekens, Benjamin Van Camp, Ahmed Mahmoud, Rishabh Nagarkar, Bart Dierickx, Karl Haugholt, Baard Nossum, Havard Torring, and Anders Hansen

Precision Time Meters for Ground and Space Applications 309
Jurijs Jonass, Vladimirs Bespal'ko, and Vjaceslavs Lapkovskis

Validation of Aeolus Wind Product at Cruzeiro do Sul-Brazil 319
Alexandre Calzavara Yoshida, Fábio Juliano da Silva Lopes, Patricia Cristina Venturini, Alexandre Cacheffo, Juan Luis Guerrero-Rascado, and Eduardo Landulfo

Lidar-Radar Synergy for the Study of Cirrus Clouds from Current Space-Based Remote Sensing: Insights for the Upcoming EarthCARE Mission 329
Carmen Córdoba-Jabonero, Álvaro Jara-Piqueras, Clara Violeta Carvajal-Pérez, Javier Carrero-González, María Ángeles López-Cayuela, Michaël Sicard, Patric Seifert, and Juan Luis Guerrero-Rascado

Scientific Challenges for Lidar-Based Dust and Ice Cloud Characterization on Mars 335
Carmen Córdoba-Jabonero, Laura Gómez-Martín, Juan José Jiménez-Martín, James A. Whiteway, Daniel Toledo, Alberto Martín-Ortega, Eamonn McKernan, Isaías Carrasco-Blázquez, Margarita Yela, and Ignacio Arruego

Ground-Based Radar Capabilities at Granada (Spain) to Support EarthCARE Mission 343
Matheus Tolentino da Silva, M. J. Granados-Muñoz, J. A. Bravo-Aranda, L. Alados-Arboledas, and J. L. Guerrero-Rascado

Comparative Analysis of Aeolus Satellite Mission L2A, L2B and L2C Products with Ground-Based Lidars: Multi-Year Cal/Val Activities in Granada, Spain 353
Jesús Abril-Gago, Pablo Ortiz-Amezcua, Juana Andújar-Maqueda, Juan Antonio Bravo-Aranda, María José Granados-Muñoz, Francisco Navas-Guzmán, Lucas Alados-Arboledas, and Juan Luis Guerrero-Rascado

Injection-Free and Cavity Free Parametric Sources for Future Spaceborne DIAL Based on Periodically Poled Nonlinear Materials 363
Jean-Baptiste Dherbecourt, Kjell Martin Mølster, Antoine Zheng, Valdas Pašiškevičius, Jean-Michel Melkonian, Michael Strotkamp, Jan Fabian Geus, Xavier Délen, Patrick Georges, S. Duzellier, Antoine Godard, and Myriam Raybaut

LiDAR Technologies and Detector Solutions 373
Jérôme Pratlong

The NASA HSRL Pathfinder Mission Concept

Chris Hostetler, John Smith, Richard Hare, Amin Nehrir, Shane Seaman, Anthony Notari, Richard Ferrare, Sharon Burton, Kathleen Powell, Tyler Thorsen, Mark Vaughan, Johnathan Hair, Robert Holz, Willem Marais, Edwin Eloranta, and Fran Fitzpatrick

Abstract The High-Spectral-Resolution Lidar (HSRL) Pathfinder Mission concept is designed to provide HSRL measurements at 532 nm and elastic backscatter lidar measurements at 1064 nm. The instrument is based on Clio, the HSRL that was descoped from NASA's Atmosphere Observing System (AOS) mission due to cost constraints. The NASA Langley Research Center (LaRC) developed the HSRL Pathfinder concept as an example of a lower-cost mission to advance the technology and demonstrate the measurement capability originally planned for AOS. Cost savings are achieved via a Class-D instrument development approach and some reductions in performance from the original Clio design. Despite these changes, the HSRL Pathfinder Mission promises to provide valuable observations for advancing studies of aerosol and cloud radiative effects, cloud microphysics, aerosol-cloud interaction, aerosol transport and speciation, and air quality. The design also enables scientifically important observations of depth-resolved ocean subsurface optical properties, snow water equivalent, and seasonal sea ice, making HSRL Pathfinder a truly multifunctional lidar mission.

Keywords High-spectral-resolution lidar (HSRL) · Ocean lidar · Aerosols · Clouds · Air quality

C. Hostetler (✉) · J. Smith · R. Hare · A. Nehrir · S. Seaman · A. Notari · R. Ferrare · S. Burton · K. Powell · T. Thorsen · M. Vaughan · J. Hair
NASA Langley Research Center, Hampton, VA 23681, USA
e-mail: chris.a.hostetler@nasa.gov

R. Holz · W. Marais · E. Eloranta
Space Science and Engineering Center, University of Wisconsin, Madison, WI 53706, USA

F. Fitzpatrick
Fibertek, Inc, Herndon, VA 20171, USA

U. N. Singh et al. (eds.), *Space-based Lidar Remote Sensing Techniques and Emerging Technologies*, Springer Aerospace Technology,
https://doi.org/10.1007/978-3-031-53618-2_1

1 Introduction

Lidar has long been an essential remote sensing tool for acquiring vertically resolved observations of aerosols and clouds. The 17-years record of the Cloud-Aerosol Lidar with Orthogonal Polarization (CALIOP) elastic backscatter measurements from the Cloud-Aerosol Lidar and Infrared Pathfinder Satellite Observations (CALIPSO) satellite has been used for many ground-breaking studies of aerosol transport, cloud distribution and microphysics, and the impacts of aerosols and clouds on the Earth's radiation budget [1]. In addition, CALIOP demonstrated that spaceborne lidar can provide scientifically valuable observations of ocean subsurface ecosystems [2].

The chief deficiency of the elastic backscatter lidar technique is the inability to provide independent measurements of particulate backscatter and extinction. The high-spectral-resolution lidar (HSRL) approach overcomes this deficiency, with the result being a significant increase in the accuracy of particulate backscatter and extinction estimates plus higher information content for aerosol typing and characterizing ocean plankton communities. The European Space Agency recognized the value of this advanced architecture two decades ago and is preparing to launch an HSRL on the Earth Clouds, Aerosols and Radiation Explorer mission in 2024. The China National Space Agency started much later but succeeded in launching an HSRL on their Atmospheric Environment Monitoring Satellite in 2022. Since 2000, NASA has funded the development and deployment of several airborne HSRLs and the advancement of spaceborne HSRL technologies. An HSRL was originally included in NASA's AOS-Sky mission concept but was later descoped due to cost constraints. Subsequently, NASA LaRC has been tasked with developing a concept for an HSRL technology demonstration mission that can be implemented at a lower cost than the HSRL originally planned for AOS. This new concept is called the HSRL Pathfinder and is described in the following sections.

2 Mission Overview

The HSRL Pathfinder mission is designed to reduce cost as much as practical while still providing significant scientific advances in measurements of aerosols, clouds, and ocean ecosystems. The baseline approach for the spacecraft is a powered Evolved Expendable Launch Vehicle Secondary Payload Adapter (ESPA), which enables cost sharing via hosting of additional payloads on the powered ESPA bus and shared launch with other payloads in the launch stack. Cost savings are also achieved by using a Class-D development strategy, which eliminates redundant components, reduces subsystem prototyping, and targets shorter duration missions. The required mission lifetime for HSRL Pathfinder is 1 year; however, expendables on the spacecraft will enable a lifetime greater than 3 years. The concept is designed for a 450-km sun-synchronous orbit, consistent with current plans for the AOS-Sky orbit, should the opportunity arise to launch into formation with AOS-Sky. Other altitudes can be accommodated, albeit with potential impacts to mission life and measurement precision.

3 Instrument Description

Figure 1 provides a high-level block diagram of the HSRL Pathfinder instrument and Table 1 lists key specifications. To fit within the volume and mass constraints of a powered ESPA bus, the transmitter is single-string, and the telescope is limited to 0.8-m in diameter. HSRL and polarization measurements are made at 532 nm only, and total elastic backscatter measurements are made at 1064 nm. The sections below describe the laser, interferometer, and detector subsystems that have been the focus of our recent technology and engineering maturation efforts.

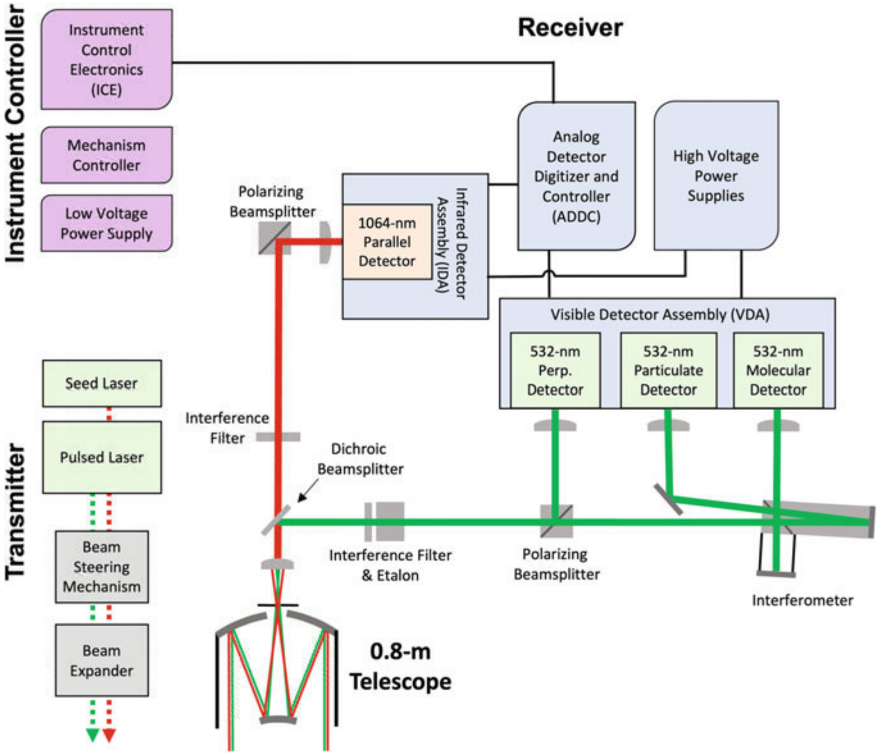

Fig. 1 High-level block diagram of the HSRL Pathfinder instrument

Table 1 Laser optical performance requirements

Parameter	Specification
Laser	
Pulse energy	125 mJ at both 532 and 1064 nm
Repetition rate	71.4 Hz (100-m along track profiling)
Pulse width	15 ± 5 ns
Spectral linewidth	< 100 MHz at 532 nm
Frequency jitter	10 MHz (1-σ)
Spectral purity	2500:1
Wavelength tunability	± 2 GHz at 532 nm
Receiver	
Telescope diameter	0.8 m
Field of view	208 μrad
Solar filtering	532 nm: 20-pm FWHM etalon 1064 nm: interference filter
HSRL optical filter	Michelson interferometer
Detectors	532 nm: Hamamatsu R9880-20 1064 nm: Excilitas APD
Detection approach	Analog + photon counting
Vertical sampling	Fundamental sampling: 120 MHz (1.25 m)

3.1 Laser

The laser is being developed by Fibertek, Inc., and is based on an injection-seeded master-oscillator power-amplifier (MOPA) architecture that has been successfully demonstrated on airborne lidars, including NASA LaRC's HSRL-2, which has flown on numerous field deployments since 2012 [3]. In 2015, Fibertek began modifying this design for spaceflight. During the design progression, a prototype of the optical module was built to evaluate operating performance and lifetime and is shown in Fig. 2. The physical configuration of the laser subsystem is partitioned into two modules: a pressurized housing which contains all optical assemblies and a vented electronics module providing power and control. The 0.2 A 0.3 × 0.5 m^3 housing contains an integral midplane that serves as the primary optical bench. The entire assembly is conduction-cooled to an external interface.

The nonplanar ring resonator is seeded with 25 mW of optical power and uses a Nd:YAG slab gain head to generate 35 mJ of nearly bandwidth-limited 15-ns optical pulses at 1064 nm with a beam quality of 1.2 M^2. Cavity locking to the seed is accomplished with a ramp-and-fire technique using two actuators, a fast electro-optic modulator and a slower PZT, to acquire and maintain resonance. Results of initial frequency stability measurements in a laboratory environment are shown in

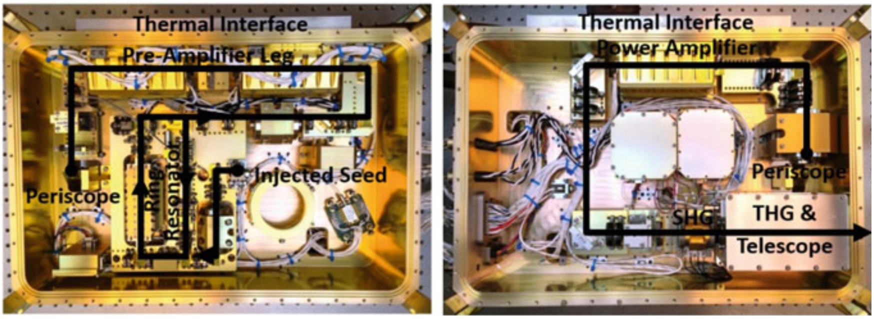

Fig. 2 Left: the upper housing compartment containing the injected seed leg, ring resonator and pre-amplifier stages. Right: the lower housing compartment containing the power amplifier and the conversion assemblies to the second and third harmonics. (This prototype was developed for a precursor program that also included 355 nm output. HSRL Pathfinder requires output at only 532 and 1064 nm.)

Fig. 3. There is no secondary spatial or axial mode content above the –35 dB level, and both short- and long-term frequency jitter with respect to the seed is maintained within <5 MHz (1σ).

The resonator output is preamplified in a pair of identical Nd:YAG slabs to produce an output of 175 mJ with 1.7 M^2. The beam is then periscoped to the other side of the midplane where it undergoes resizing and subsequent amplification to 275 mJ with 2.2 M^2. Type I mixing in lithium triborate (LBO) is used to convert to the second harmonic at 532 nm, with efficiencies up to ~70% and M^2s in the range of 2.5 to 3.0.

After characterization of the laser performance, the prototype was subjected to a 3×10^9 shot (equivalent to 1.3 year @ 71 Hz) life test to evaluate component performance over extended operation, the suitability of manufacturing processes to limit material outgassing contamination, and component fatigue over extended operation. While the test showed very little optical wear due to contamination, shortcomings were noted in the life of the pump diodes and the cavity locking algorithm under

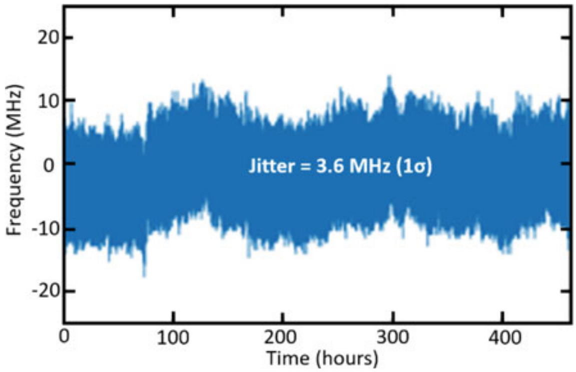

Fig. 3 Frequency jitter of the pulsed output with respect to the seed laser

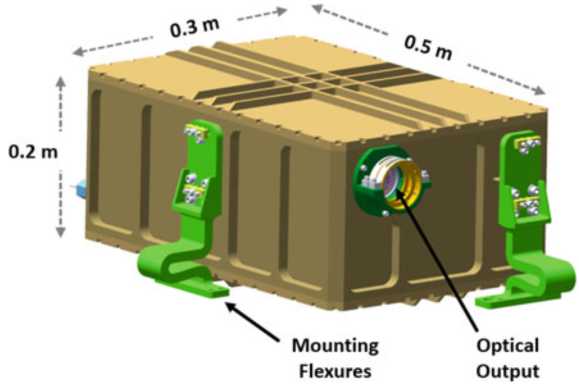

Fig. 4 Configuration of the flight laser optical module

certain, extremely low-probability events. Recent development work has led to the closure of these two risk items. Pump diodes from two vendors have been life tested at NASA LaRC to >6.6×10^9 shots (equivalent to 3 years at 71 Hz), with power degradation of only 0.5% per billion shots, and corrections to the locking algorithm have been successfully demonstrated.

With these positive results, detailed design of the flight laser optical and electronics modules has begun. Figure 4 shows the current configuration of the laser optical module. Current work is focusing on the structural, thermal, and optical analyses to ensure appropriate margins have been met for surviving the launch environments. An example is the design of mounting flexures that shift higher frequency energy to below the resonant frequency of the midplane optical bench and internal subassemblies. Component load information is then used to ensure the component designs support required margins.

3.2 HSRL Interferometric Optical Filter

The instrument concept employs a field-widened, off-axis Michelson interferometer to separate 532-nm molecular and particulate backscatter [4]. Field-widening enables accommodation of a wide range of field angles without compromising performance. Tilting slightly off axis enables capturing the back-reflected light in addition to the traditional Michelson output, thereby providing a second measurement channel. The laser transmitter is tuned to provide destructive interference of particulate backscatter on the Molecular Channel output and constructive interference on the Particulate Channel output. Through appropriate choice of the free spectral range, the molecular backscatter is distributed equally between the two channels. Figure 5 shows the spectral distributions of the interferometer input and outputs. LaRC has used this Michelson approach on HSRL-2 for 355-nm measurements on numerous airborne field deployments since 2012 [3]. In a prior development effort, a prototype 355-nm interferometer designed for spaceflight was environmentally tested to TRL-6 in 2018.

Figure 6 shows the prototype interferometer subsystem that is currently undergoing TRL-6 testing at NASA LaRC. The design includes a 50:50 beam splitter cube that divides the input light equally between the two interferometer arms. One arm is solid fused silica glass with a high-reflection coating on the end. In the other arm, the beam travels in free space to a high-reflector mirror mounted on a metering structure. The tuning of the interferometer was made insensitive to temperature by

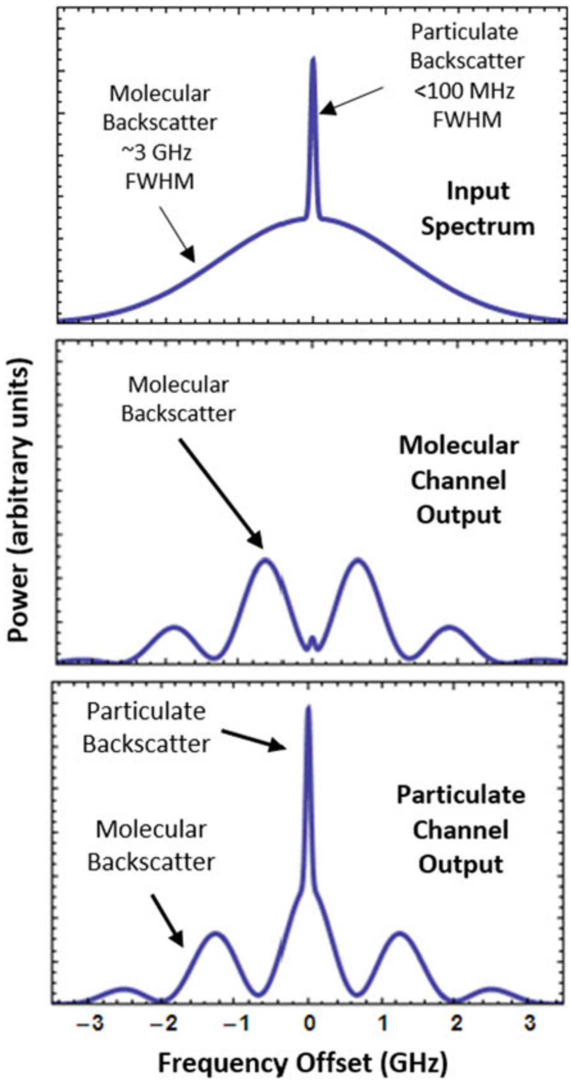

Fig. 5 Top: input spectrum. Middle (Bottom): portion of spectrum incident on the Molecular Channel (Particulate Channel) detector

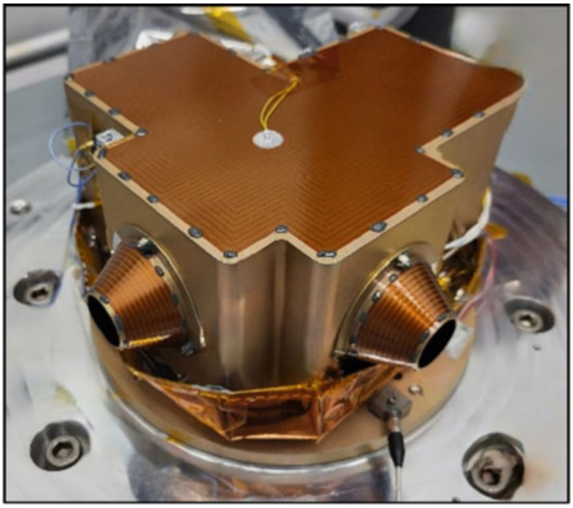

Fig. 6 Interferometer subsystem enclosed in thermal housing. Heaters are integrated to cover plates to precisely control temperature

designing the coefficient of thermal expansion of the metering structure to compensate for temperature-induced changes in the refractive index and length of the glass in the solid arm. Through structural-thermal-optical performance modeling, many variations of this metering structure were analyzed to determine the optimum design that imparts minimal distortion and gravity sag on the end mirror.

Implementation of the HSRL technique requires the interferometer and laser to remain spectrally aligned. Interferometer tuning drift is considered inevitable, requiring the laser to be episodically retuned to achieve optimal constructive and destructive interferences on the two outputs. The operational goal is to avoid retuning the laser to the interferometer more frequently than once every two weeks. Long-term stability testing (Fig. 7) shows that the as-built prototype meets this metric.

3.3 Detection Subsystems

To conserve cost, the 532-nm detection subsystem is based on that used on CALIOP, but with significant improvements. The baseline detectors are Hamamatsu metal-packaged R9880-20 photomultiplier tubes (PMTs). These PMTs are inherently rugged and extensive testing has shown these tubes to be superior to the PMTs used on CALIOP in several ways, including quantum efficiency, transient recovery, and gain stability. NASA LaRC has developed and tested a novel electronics design to process the PMT signals. It is based on an analog detection architecture and achieves an 8-order-of-magnitude linear dynamic range, far exceeding that of CALIOP (6 orders) [5]. The design permits fast gating to suppress the signal spike from the ocean surface reflection, thereby reducing artifacts in the ocean subsurface signal.

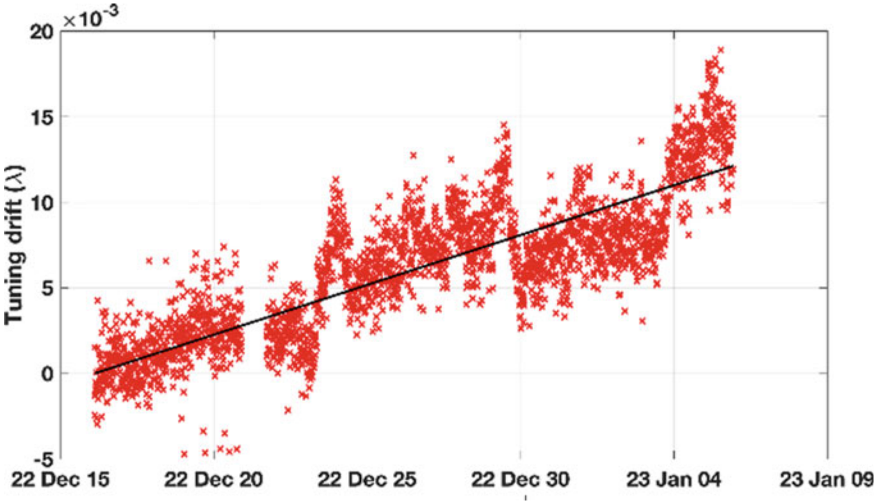

Fig. 7 Long-term (20-day) frequency drift measurements of the prototype interferometer scaled in wavelengths at 532 nm. The trend (black line) is 4×10^{-3} lambda/week, well within the requirement of $<1 \times 10^{-2}$ lambda/week

The fundamental sampling period is 120 MS/s, which equates to a sampling resolution of 1.25 m (~1 m in the ocean), also far exceeding the 30-m resolution of CALIOP. Samples will be averaged to coarser resolutions in the atmosphere, and resolutions may vary with altitude to reduce downlink volume. The objective is to provide 1-m resolution for ocean, snow, and sea-ice profiling and 5-m resolution at lower altitudes to enable advanced retrievals of extinction in low-altitude water clouds. All profile data will be downlinked at single-shot resolution, resulting in 100-m spacing of profiles along the ground track.

The signals from each PMT are read by three 14-bit digitizers with overlapping dynamic ranges. A field programmable gate array (FPGA) performs preliminary processing required to merge the three data streams into a single profile. It also vertically averages samples as required to meet the downlink budget and formats the data for transmission to the instrument control computer, which packetizes data for downlink. Figure 8 shows a photo of the spread system that incorporates all hardware and firmware features of the design and has been used for end-to-end verification testing.

The 1064-nm detector is a low ionization ratio Excelitas Si avalanche photodiode (APD), similar to those used on the CALIOP and, more lately, the Global Ecosystem Dynamics Investigation (GEDI) lidars [6]. The HSRL Pathfinder APD will require some changes from the GEDI detectors in terms of signal coupling, transimpedance gain, bandwidth, and operating temperature, to optimize signal-to-noise ratio for atmospheric, as opposed to GEDI's vegetation canopy, measurements.

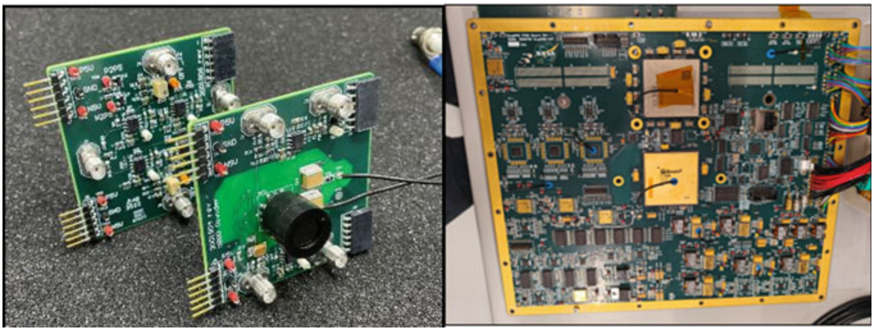

Fig. 8 Spread system of the 532-nm detection subsystem. Left: PMT and amplifier boards. Right: signal processing board incorporating digitizers and FPGAs for on-board processing. This system has undergone end-to-end testing including the injection of realistic light profiles to the PMT and processing of the acquired signals

4 Rationale for Design Choices

The most fundamental design choice is that of wavelength. We chose to operate at 532 and 1064 nm for several reasons. The first was consistency with the 17-year CALIOP data record for climate-trend studies and overall science context. The 532-nm wavelength also provides good contrast between aerosol and molecular backscatter, enabling accurate HRSL retrievals at low aerosol loading levels and transmits sufficiently through water to enable ocean subsurface profiling. The 1064-nm elastic backscatter measurement has high utility for discriminating between aerosols and clouds, which is critical to science analysis. Operating at an additional wavelength of 355 nm would be highly desirable for several reasons (continuity with EarthCARE, increase in aerosol microphysical information, etc.) and was included on an earlier concept developed jointly with the French national laboratories and CNES, but doing so is not practical for the HSRL Pathfinder due to cost.

The choice of the field-widened Michelson interferometer as the HSRL receiver filter was driven by several factors. First, it enables a high degree of separation of particulate backscatter between the HSRL channels. Our goal for the Contrast Ratio (ratio of particulate backscatter in the Particulate and Molecular Channels) is 50:1. A high Contrast Ratio reduces the impact of errors in the calibration of particulate backscatter crosstalk between the HSRL channels, making aerosol retrievals more accurate and extending the dynamic range over which HSRL retrievals are possible to a significant fraction of cirrus clouds. Second, the Michelson approach enables the molecular backscatter crosstalk between the two HSRL channels to be known a priori by choosing a free spectral range that delivers 50% of the molecular backscatter to each channel regardless of the backscatter volume's temperature. Third, the field widening allows for larger etendues, e.g., larger telescope diameters for higher signal collection and/or larger fields-of-view and laser divergences to address eye-safety. It also allows the design to be vetted on airborne HSRLs, which tend to have higher etendues than space HSRLs. Forth, the design parameters can be optimized to enable ocean profiling with no compromise to atmospheric retrievals.

The detection subsystem design choices were driven by cost, risk, and performance considerations. CALIOP heritage was leveraged as far as possible to control cost and risk. The CALIOP-like approach at 1064-nm, with Si APDs and analog readout, enables improvements over CALIOP's proven performance without significant modifications to existing designs. The 532-nm detection subsystem also has much in common with the CALIOP design but includes more modifications, in terms of higher performing PMTs and improvements in the readout and signal processing electronics, that significantly increase science capability. The improvements enable advanced retrievals of water cloud optical properties, depth-resolved ocean optical properties, snow depth, and seasonal sea ice thickness.

5 Science Outlook

The science rationale for implementing HSRL measurement capability in the HSRL Pathfinder and our original Clio HSRL concept for the AOS-Sky mission is an improvement in accuracy and information content over elastic backscatter lidar for aerosol observations. In the case of backscatter lidar, accuracy can be poor due to the a priori assumption of the particulate extinction-to-backscatter ratio in the profile retrieval (i.e., barring an external constraint, like optical depth, which enables a column-average estimate of lidar ratio but not the lidar ratio profile [see Fig. 9]). The resulting error in retrieved particulate backscatter and extinction accumulates as the retrieval proceeds downward through the atmosphere to the surface, resulting in the largest errors at the surface, where the highest concentration of aerosol is often located. The HSRL retrieval requires no such error-prone assumptions and is thereby much more accurate.

Along with high accuracy, a critically important feature of the HSRL measurement is that the data products are inherently more suitable to model assimilation. The uncertainties in elastic backscatter lidar particulate extinction and backscatter profiles are difficult to quantify due to the accumulation of unknown bias errors, making those profiles unsuitable for assimilation. The HSRL product uncertainties are quantifiable, and the data are therefore well-suited for assimilation. Many future science advances will rely on assimilation of profile data into reanalysis models and weather and air quality forecast models, hence model compatibility is of paramount importance.

The HSRL Pathfinder's ability to retrieve extinction-to-backscatter ratio, in addition to the depolarization and backscatter color ratios demonstrated with CALIOP, will provide significantly greater information content for aerosol typing [7] (e.g., smoke vs. marine as illustrated Fig. 9), which is important for aerosol source attribution and air quality studies.

Advanced cloud measurements are another important objective of the HSRL Pathfinder. Cloud retrievals can be made using algorithms like those used on CALIOP data via combining the signals from the Particulate and Molecular Channels. Doing

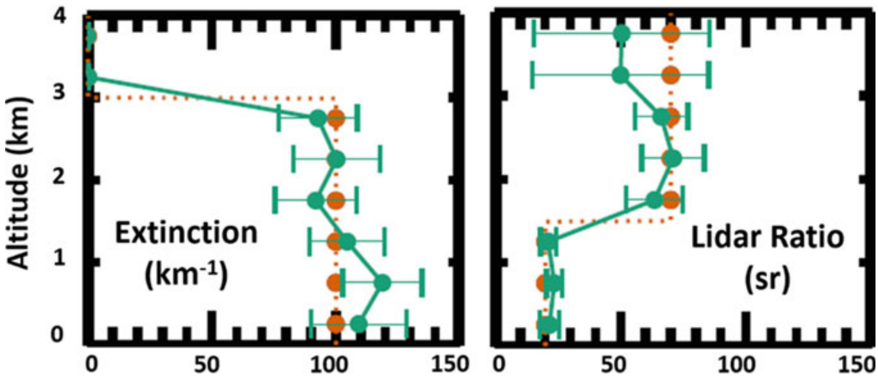

Fig. 9 Simulation realization for a smoke layer overlying a marine boundary layer (simulation in green, truth in orange). The Lidar Ratio clearly shows the boundary between the layers. For this scene, the vertical and horizontal averaging resolutions were 500 m and 50 km, respectively

so makes HSRL Pathfinder functionally similar to CALIOP but with much higher signal-to-noise performance. The higher vertical resolution and linearity of the 532-nm detection system will expand capability significantly by enabling estimates of cloud extinction profiles to a few 10 s of meters into the tops of water clouds [8] and, when combined with droplet size information from other sensors (e.g., polarimeters), cloud droplet number density [9]. While interferometric HSRL techniques are severely challenged for retrievals of strongly scattering cloud, the high Contrast Ratio of our interferometer should enable HSRL retrievals of a significant fraction of cirrus clouds, providing unprecedented accuracy in estimates of cirrus optical properties key to estimating the radiative impact of cirrus.

The high vertical resolution and linearity of the 532-nm detection system make the lidar truly multifunctional. High resolution HSRL measurements in the near-surface ocean enable independent and accurate measurements of particulate (i.e., phytoplankton) backscatter and diffuse attenuation coefficient, in turn leading to depth-resolved estimates of marine biomass and net primary productivity [10]. While the measurement lacks swath, the retrievals are much more direct than passive ocean color retrievals, are immune to overlying atmospheric conditions (e.g., strong aerosol layers, optically thin clouds), and can be acquired at night as well as during day. HSRL Pathfinder observations would enhance the value of the entire ocean color data record by assessing ocean color retrievals and training advanced ocean color algorithms. The high vertical resolution will enable estimates of snow depth, as recently demonstrated with data from the second-generation Ice, Cloud and land Elevation Satellite (ICESat-2) [11], and Brillouin scattering measurements from the Molecular Channel may enable estimates of snow density. Additionally, high vertical resolution plus Brillouin scattering measurements should enable entirely new retrievals of seasonal sea ice thickness.

In summary, HSRL Pathfinder's multifunctional capabilities would enable several scientifically significant advances. HSRL Pathfinder would provide advanced aerosol and cloud observations relevant to air quality and weather applications and climate science, unprecedented measurements of ocean optical properties for ocean ecosystems studies, more accurate estimates of snow water equivalent to better understand terrestrial hydrology and its response to climate change, and estimates of seasonal sea ice thickness to improve understanding of sea-level rise and cryosphere-atmosphere interaction.

References

1. Stephens G, Winker D, Pelon J, Trepte C, Vane D, Yuhas C, L'ecuyer T, Lebsock M (2018) CloudSat and CALIPSO within the A-Train: ten years of actively observing the earth system. Bull Am Meteor Soc 99(3):569–581
2. Behrenfeld MJ, Hu Y, Bisson KM, Lu X, Westberry TK (2022) Retrieval of ocean optical and plankton properties with the satellite Cloud-Aerosol Lidar with Orthogonal Polarization (CALIOP) sensor: background, data processing, and validation status. Remote Sens Environ 281:113235
3. Burton SP, Hostetler CA, Cook AL, Hair JW, Seaman ST, Scola S, Harper DB, Smith JA, Fenn MA, Ferrare RA, Saide PE (2018) Calibration of a high spectral resolution lidar using a Michelson interferometer, with data examples from ORACLES. Appl Opt 57(21):6061–6075
4. Seaman ST, Cook AL, Scola SJ, Hostetler CA, Miller I, Welch W (2015) Performance characterization of a pressure-tuned wide-angle Michelson interferometric spectral filter for high spectral resolution lidar. In: Lidar Remote Sensing for Environmental Monitoring XV Proceeding of SPIE. 9612:96120H
5. Hunt WH, Winker DM, Vaughan MA, Powell KA, Lucker PL, Weimer C (2009) CALIPSO lidar description and performance assessment. J Atmos Oceanic Tech 26(7):1214–1228
6. Sun X, Blair JB, Bufton JL, Faina M, Dahl S, Bérard P, Seymour RJ (2020) Advanced silicon avalanche photodiodes on NASA's global ecosystem dynamics investigation (GEDI) mission. In: Photonic Instrumentation Engineering VII Proceeding of SPIE 11287:1128713
7. Burton SP, Ferrare RA, Hostetler CA, Hair JW, Rogers RR, Obland MD, Butler CF, Cook AL, Harper DB, Froyd KD (2012) Aerosol classification using airborne high spectral resolution Lidar measurements–methodology and examples. Atmosp Meas Techn 5(1):73–98
8. Roy G, Cao X (2010) Inversion of water cloud lidar signals based on accumulated depolarization ratio. Appl Opt 49(9):1630–1635
9. Grosvenor DP, Sourdeval O, Zuidema P, Ackerman A, Alexandrov MD, Bennartz R, Boers R, Cairns B, Chiu JC, Christensen M, Deneke H (2018) Remote sensing of droplet number concentration in warm clouds: a review of the current state of knowledge and perspectives. Rev Geophys 56(2):409–453
10. Hostetler CA, Behrenfeld MJ, Hu Y, Hair JW, Schulien JA (2018) Spaceborne lidar in the study of marine systems. Ann Rev Mar Sci 10:121–147
11. Hu Y, Lu X, Zeng X, Stamnes SA, Neuman TA, Kurtz NT, Zhai P, Gao M, Sun W, Xu K, Liu Z (2022) Deriving snow depth from ICESat-2 LiDAR multiple scattering measurements. Front Rem Sens 3:855159

25 Years of CALIPSO

David Winker

Abstract Selected for development in 1998 and launched together with CloudSat in 2006, the Cloud-Aerosol Lidar and Infrared Pathfinder Satellite Observations (CALIPSO) mission terminated science operations in the summer of 2023 after completing 17 years of on-orbit observations. As one of NASA's Earth System Science Pathfinder missions, CALIPSO was truly a pathfinder. CALIPSO observations provided a new perspective on clouds and aerosol and have not only met but far exceeded the original objectives of the mission. Many unanticipated findings and data applications have been discovered along the way. Flying with many other remote sensing instruments, as part of the A-train constellation, stimulated the discovery of numerous retrieval synergies between lidar and other sensors. This paper describes how the CALIPSO mission came to be, discusses some of the early choices made by the CALIPSO team that shaped the mission, and some of the challenges facing the team in developing the first-ever global climatologies of aerosol and cloud based on lidar observations.

Keywords Space lidar · Active remote sensing · Clouds · Aerosols

1 Introduction

The Cloud-Aerosol Lidar and Infrared Pathfinder Satellite Observations (CALIPSO) mission began with the selection of the Step-2 proposal to the NASA Earth System Science Pathfinder (ESSP) program in December 1998. The 3rd International Workshop on Space-Based Lidar Remote Sensing Techniques and Emerging Technologies was held in June 2023, just after CALIPSO completed 17 years of observations and a few weeks before the planned termination of CALIPSO payload operations. Therefore the Workshop was an appropriate time to take a retrospective look at how CALIPSO came to be and highlight a few of the challenges and a few of the

D. Winker (✉)
Science Directorate, NASA Langley Research Center, Hampton, VA 23681, USA
e-mail: david.m.winker@nasa.gov

U. N. Singh et al. (eds.), *Space-based Lidar Remote Sensing Techniques and Emerging Technologies*, Springer Aerospace Technology,
https://doi.org/10.1007/978-3-031-53618-2_2

many achievements. More than a decade of global cloud and aerosol profiling, collocated with many other remote sensing observations from the A-train constellation, has revolutionized the way aerosol and cloud studies are done, and provided new ways of evaluating models. CALIPSO broke new ground in many areas, forcing the CALIPSO team to creatively address many challenges.

2 CALIPSO Grew from LITE

The Earth Observing System (EOS), consisting of the Terra, Aqua, and Aura satellites was conceived in the 1980's, developed in the 1990's, and launched between 1999 and 2004. The initial vision included an advanced lidar for ozone and water vapor profiling, which was later descoped along with a number of other sensors due to cost.

Meanwhile, the Lidar In-Space Technology Experiment (LITE) was developed as a three-wavelength (1064/532/355 nm) backscatter lidar by NASA Langley Research Center (Langley), beginning in the late 1980's. LITE flew on the NASA Space Shuttle STS-64 mission in September 1994 [1]. LITE only acquired 53 h of observations during the 2-week mission of STS-64 but provided our first global-scale view of cloud and aerosol from a lidar perspective. LITE gave us our first view of atmospheric structure on a global scale and observed parts of the globe never seen by lidar before. Dense clouds block lidar signals but LITE showed that the global coverage of dense clouds blocking the beam was much less than expected. LITE also observed the vertical distribution of aerosol on a global scale for the first time.

LITE was developed as a technology demonstration but also served as a proof of concept that a satellite lidar could provide unique and essential observations of aerosol and clouds. In addition, the successes of LITE motivated NASA to begin exploring the possibilities of a free-flying lidar satellite. The NASA Earth System Science Pathfinder (ESSP) program was initiated in the mid-1990's to fly relatively small science missions to fill gaps in the global observing system. Immediately following the LITE mission, design studies of a free-flying lidar to study the global distribution and properties of clouds and aerosols were begun at Langley, targeting the new ESSP program.

Around that time, a joint Langley-JPL workshop was held to discuss possibilities for a satellite mission involving a cloud profiling W-band (94 GHz) radar and an elastic backscatter lidar, due to the realization that the combined capabilities of lidar and W-band radar were necessary to address the need for vertical profiling of cloud occurrence and water/ice mass distributions. Similar discussions were happening at about the same time in Europe [2], which ultimately resulted in the ESA EarthCARE mission [3]. Initial discussions with JPL envisioned an ESSP mission carrying a backscatter lidar, W-band radar, and several passive sensors. In the end the radar and lidar were proposed to ESSP as separate missions due to the cost cap on individual ESSP missions.

A lidar proposal was submitted in 1996 but was unsuccessful, primarily due to cost issues. Looking forward to the next ESSP opportunity, the Langley team contacted members of the French science community and negotiated a partnership where Langley would develop a payload consisting of a two-wavelength, depolarization lidar (Cloud-Aerosol Lidar with Orthogonal Polarization, CALIOP, rhymes with eye-oh-pea), a Wide Field Camera (WFC) with a single visible channel, based on a star tracker from Ball Aerospace Technologies Corporation (BATC) and fulfilling the function of the film camera flown on LITE, a payload controller, and an X-band transmitter to downlink science data [4]. The Centre National d'Etudes Spatiale (CNES) was to provide a PROTEUS spacecraft and an infrared imaging radiometer (IIR), reducing the mission cost to NASA to within the ESSP cost cap. The IIR was a compact instrument, built by SODERN (Paris), based on a new technology 2D bolometer array and matching much of the capability of the MODIS infrared channels in a much smaller package. BATC was prime contractor for the payload and fabricated CALIOP, except for the detectors and detector electronics which were designed and built at Langley. This second CALIPSO proposal was selected in December 1998, with the CloudSat proposal selected in 1999 after additional analysis was performed.

3 Early Decisions

Analysis of the LITE laser after STS-64 returned to Earth showed significant contamination-induced laser damage due to the 355 nm laser light. To reduce laser technical risk, it was decided that the CALIOP laser would only operate at 1064 nm and 532 nm but there was a desire to do something new, beyond LITE. At the time there were few polarization lidars but Ken Sassen had recently published a paper in the Bulletin of the American Meteorological Society pointing out the utility of lidar depolarization measurements [5]. A decision was made that the CALIOP laser would transmit a highly linearly polarized beam and the lidar receiver would have co-polar and cross-polar 532 nm channels.

Following on the experience from LITE, we realized there were a number of design challenges in moving from a two-week experiment on the Space Shuttle to an extended mission on a free flyer. LITE was based on a water-cooled, flashlamp pumped laser. The CALIOP laser would have to be passively cooled and laser lifetime was a major concern since the flight lasers were required to have a design lifetime of 3 billion shots. Diode-pumped lasers were new at the time and laser pump diodes were not as reliable as they are now. Laser damage from contamination was also a concern and the laser would need a ruggedized design to survive G-forces during launch. Because of laser risk concerns raised over the first proposal, a prototype of the flight laser was fabricated and life testing was begun in time to include results in the proposal to ESSP to demonstrate the reliability of the design. The Risk Reduction Laser (RRL) [6] was jointly conceived by Langley and BATC and developed by Fibertek Inc. in collaboration with experts from Langley and BATC. Fabrication of the RRL began about a year before the proposal to ESSP was due. The RRL was based on prior lasers designed for field deployment, but output power was derated by a factor of two from the design values to promote long lifetime. Peak optical power of the laser pump diodes was derated significantly from their design values and power density in the Nd:YAG slab was a small fraction of the damage threshold. Prior experience at Fibertek indicated that operation in an atmosphere containing oxygen reduced contamination risk relative to operation in a vacuum so the flight lasers were designed to operate inside a canister pressurized to just over 1 bar with dry air. A comprehensive contamination control plan was developed before fabrication began. The RRL was fabricated and was 50 million shots into an extended life test when the second proposal was submitted in 1998. The RRL was eventually operated for 1.2 billion shots (about 2 years) with only a 4% decrease in pulse energy, verifying the reliability of the design and the success of the contamination control procedures developed to avoid contamination damage.

There is always a desire to fly active sensors in a low orbit, to maximize signal-to-noise ratio (SNR), and fortunately LITE flew on STS-64 at 260 km altitude. There was initial discussion of flying CALIPSO as low as possible. With a primary science objective of better characterizing the impacts of aerosols and clouds on Earth's radiation budget, the CALIPSO science team identified numerous advantages of flying in formation with the EOS-PM satellite (later renamed EOS Aqua) which was to carry MODIS and CERES. The EOS science strategy was for MODIS to observe aerosols and clouds and for CERES to use MODIS cloud observations in its task of measuring broadband radiative fluxes at the top of the atmosphere. Formation flying of CALIPSO with CloudSat was always a key desire, which would not only allow the profiling of virtually all clouds but also enable joint retrievals of cloud properties. The driving synergy with CERES was the ability to use collocated CALIOP and CloudSat profiles of cloud vertical structure in the CERES flux retrieval algorithms. Flying in formation with Aqua, CALIOP could also provide validation of MODIS cloud masking and cloud retrievals [eg: 7] and MODIS would provide context for the CALIOP curtains of cloud and aerosol observations. In the end, the science team felt the synergies of flying with Aqua at 705 km outweighed the increase in SNR that could have been achieved in a lower orbit and the CloudSat team was convinced to also fly at 705 km. As the A-train developed—adding Aura, POLDER, and OCO-2—many more synergies were realized.

Formation flying of CALIPSO and CloudSat was a further challenge. At the time, flying in close formation had not been attempted for Earth remote sensing satellites and some cast doubt on its feasibility. But JPL successfully developed procedures to control the CloudSat spacecraft to fly to CALIPSO with an along-track separation of 12–15 s, while minimizing the cross-track differences between the CPR and CALIOP footprints. The impact of these collocated radar-lidar cloud observations on our understanding of global clouds was called out in the Fifth Assessment Report of the Intergovernmental Panel on Climate Change (IPCC).

4 Challenges and Innovations

Calibration of the lidar attenuated backscatter returns was to be performed using the atmospheric normalization technique, based on molecular backscatter found above the stratospheric Junge aerosol layer. This technique references lidar returns from the mid-stratosphere to molecular density profiles derived from global re-analysis products, essentially using the molecular atmosphere as a calibration target, and had been used for decades on ground-based lidars [8]. Therefore, the lidar was required to accurately measure weak signals from high altitude molecular backscatter returns, but there was also a requirement to measure the backscatter signals from strongly scattering liquid clouds. This required the analog detection system to have a highly linear dynamic range of six orders of magnitude [9]. This technical challenge was met by Langley engineers.

Calibration was initially performed using lidar returns from 30 to 35 km altitude, but careful analysis showed that aerosol concentrations in the tropical stratosphere, while low, were enough to cause significant calibration errors which propagated into CALIOP retrievals. Therefore, starting with Version 4 data products, the calibration region was raised to 35 to 40 km. Raising the altitude required a major change to the Level 1 calibration software as substantially greater averaging was required to maintain the same calibration precision and CALIOP adopted cross-track averaging for the first time [10]. Subsequent analysis has shown the Version 4 calibration has excellent long-term stability. The red curve in Fig. 1 shows a time series of CALIOP 532 nm attenuated backscatter integrated from 25 to 40 km, where the lidar backscatter is dominated by molecular scattering, and averaged over 50°S–50°N. The blue dashed curve is the normalized molecular number density from the MERRA-2 re-analysis product, interpolated to the CALIPSO ground track, over the same altitude range. The black curve shows the time history of 532-nm laser pulse energy over the mission. Changes in pulse energy over the mission were dominated by the loss of pump diodes and a switch between primary and backup lasers in March 2009. The apparent dip in laser energy after 2020 is likely due to a degradation of the laser energy sensor. It is apparent the calibration scheme is able to accurately account for these variations in pulse energy and produce a stable long-term record, as demonstrated by the high correlation of stratospheric attenuated backscatter and molecular density. The discrepancy between the two in early 2022 is due to the eruption of the Hunga-Tonga volcano, which injected aerosol into the 35–40 km altitude region.

Langley had developed retrieval algorithms over several decades for a ground-based 48″ lidar, used for studies of stratospheric aerosol, and for lidars flown on airborne campaigns. Processing the data from these instruments was a relatively manual operation. Observations performed for aerosol studies were often acquired only in cloud-free conditions. CALIOP required the development of new algorithms: algorithms to detect the boundaries of cloud and aerosol layers, to automatically discriminate between aerosols and clouds, and to use the lidar signals to classify aerosol by type in order to estimate the aerosol lidar ratio needed for extinction